Cretaceous Research 105 (2020) 104073

Contents lists available at ScienceDirect

Cretaceous Research

journal homepage: www.elsevier.com/locate/CretRes

Spinicaudatans from the Yixian Formation (Lower Cretaceous) and the Daohugou Beds (Jurassic) of Western Liaoning, China

Liang Hu [a, b], Tao Zhao [c], Yanhong Pan [a, *]

[a] CAS Key Laboratory of Economic Stratigraphy and Palaeogeography, Nanjing Institute of Geology and Palaeontology and Center for Excellence in Life and Paleoenvironment, Chinese Academy of Sciences, 210008 Nanjing, China
[b] University of Chinese Academy of Sciences, China
[c] State Key Laboratory of Palaeobiology and Stratigraphy, Nanjing Institute of Geology and Palaeontology and Center for Excellence in Life and Paleoenvironment, Chinese Academy of Sciences, 210008 Nanjing, China

a r t i c l e i n f o

Article history:
Received 12 August 2018
Received in revised form
29 December 2018
Accepted in revised form 31 January 2019
Available online 6 March 2019

Keywords:
Jehol Biota
Yanliao Biota
Clam shrimps
Phosphatization
Carbonaceous remains

a b s t r a c t

The Jehol and Yanliao Biota constitute two world-famous Mesozoic lacustrine Konservat Lagerstätten. In contrast to numerous comparative studies on their different fossil assemblages, their taphonomic features have rarely been compared. Here we investigate the diagenetic pathways of spinicaudatans from the Lower Cretaceous Yixian Formation and the Jurassic Daohugou Beds to figure out whether they are similar. The specimens were categorized into eight types based on the colors of the carapaces and the characteristics of the surrounding matrix and subsequently were studied under the scanning electron microscope (SEM) and energy dispersive X-ray spectrometer (EDS). Spinicaudatan carapaces from the Yixian Formation are phosphatized lacking any traces of organic remains, whereas those from the Daohugou Beds contain a mineralized layer and a carbonaceous layer. Phosphatization apparently was a common taphonomic pathway of spinicaudatan carapaces in the Yixian Formation, while in the Daohugou Beds carbonaceous remains, probably the diagenetic products of chitin, are common. This suggests that the taphonomic environment and water chemistry, to which the Jehol and Yanliao Biota were subjected, differed.

1. Introduction

The Middle-Late Jurassic Yanliao Biota and the Early Cretaceous Jehol Biota from northeastern China represent two well-known Mesozoic Konservat Lagerstätten (Grabau, 1928; Chang et al., 2003; Zhou et al., 2003; Zhou, 2006, 2014; Benton et al., 2008; Pan et al., 2013; Sullivan et al., 2014, 2017; Xu et al., 2016; Zhou and Wang, 2017). Both biota are preserved in lacustrine deposits influenced by volcanic processes (Jiang et al., 2011, 2012, 2014; Pan et al., 2012).

Studies of the diagenetic pathways of the two biota, responsible for their exceptional preservation, are limited. Leng and Yang (2003) first discussed the important role of early pyritization in the preservation of plants and vertebrate feathers in the Jehol Biota. Wang et al. (2012) recorded pyritized Jehol insects. Pan et al. (2014) further indicated that pyrite and clay minerals are both important in the preservation of Ephemeropsis trisetalis. Additionally, microbial mats may contribute to the exceptional preservation of the Jehol Biota (Fürsich et al., 2007; Pan et al., 2012; Hethke et al., 2013), although no solid evidence has been documented so far. As for the Yanliao Biota, most fossil insects from the Daohugou Beds contain organic remains whereas only some are pyritized (Wang et al., 2008). A taphonomic comparison of the two biota based on bivalves showed that those from the Jurassic Daohugou Beds contain remains of the organic periostracum, while the ones from the Yixian Formation contain no organic material (Fürsich and Pan, 2015). Clearly, the diagenetic pathways of the two biota need to be further explored to understand their differences in preservation quality. We therefore use spinicaudatans (clam shrimps), one of the dominant invertebrate groups of both biota, to test whether they share the same diagenetic pathways, and to discuss the corresponding taphonomic environments.

2. Geological background

The Yixian Formation consists of lacustrine deposits with interbedded volcanic rocks, which unconformably rest on the Tuchengzi Formation or directly on the Precambrian basement, and

* Corresponding author.
E-mail address: yhpan@nigpas.ac.cn (Y. Pan).

https://doi.org/10.1016/j.cretres.2019.01.025
0195-6671/

are overlain by the Jiufotang Formation (Gu, 1962). Based on the lithofacies and fossil content, the Yixian Formation has been divided into four units, in ascending order: Lujiatun Unit, Lower lava Unit, Jianshangou Unit, and Upper lava Unit (Jiang and Sha, 2007; Jiang et al., 2012). Recently, Chang et al. (2017) provided high-precision $^{40}Ar/^{39}Ar$ ages (125.8 ± 1.0 Ma and 126.0 ± 0.8 Ma) for the Lujiatun Unit and recalibrated previous published ages via new age interpretations, which indicated the Lujiatun Unit was deposited more or less contemporaneously with the Jianshangou unit (Chang et al., 2017). The Lujiatun Unit is mainly composed of volcanic conglomerates, sandstones with/without conglomerates, and tuffs with lapilli (Jiang and Sha, 2007), yielding articulated vertebrate skeletons without soft tissues, and lacking invertebrates and plants (Pan et al., 2013; Zhou, 2014). The Jianshangou Unit is mainly composed of volcanic sandstones, siltstones, claystones, shales and tuffs (Jiang and Sha, 2007), yielding abundant well-preserved plants, invertebrates and vertebrates with exceptional preservation of soft tissues, such as body outlines and skin casts (Pan et al., 2013). All reported spinicaudatan fossils from the Yixian Formation are in fact from the Jianshangou Unit, which is also true of our material from the Yixian Formation (Fig. 1).

In the Early Cretaceous, the North China Craton was affected by tectonic activities, leading to the formation of many fault basins and lakes (Wu et al., 2008; Zhou, 2014). The sediments of the paleo-lake in Sihetun area are composed of wave-influenced, suspension, hyper-concentrated density-flow and turbidity-current deposits (Jiang and Sha, 2007). Based on the analysis of the remains of the eight different fossil communities on bedding planes from the Zhangjiagou and Erdaogou excavations, Pan et al. (2012) assumed that the sediments of the Yixian Formation represent a large, eutrophic, shallow lake system (Pan et al., 2012).

The Daohugou Beds are not a formal lithostratigraphic unit. Their stratigraphic position is still controversial. The beds were once placed in the Yixian Formation (Wang et al., 2000), the Jiulongshan Formation (Ren et al., 2002) or the Haifanggou Formation (Huang et al., 2015), etc. Here we follow the latest suggestion by Huang (2015, 2016) and Huang et al. (2015) that the Daohugou Beds belong to the Haifanggou Formation, and are overlain by the Tiaojishan Formation. The age of the Daohugou lavas is about 165 Ma (Middle Jurassic; Chen et al., 2004; Liu et al., 2006; Yang and Li, 2008; Meng et al., 2018). The base of the Daohugou Beds is a set of conglomerates, yielding few fossils. The middle and upper parts are composed of mudstones and siltstones interbedded with thin layered tuffs, yielding abundant fossils (Huang, 2016). The fossils studied were collected from the middle and upper parts of the beds, preserved in tuffaceous mudstones or siltstones (Fig. 1). The Yanliao paleoenvironment was poorly known except for some tentative inferences (Xu et al., 2016). The Daohugou area might have been a near-shore shallow lake based on the study of the fossil insects (Tan and Ren, 2002; Ren et al., 2010). Recently, Yang et al. (2019) recognized frequent alternations of thin lacustrine deposits and thick volcaniclastic apron deposits in the Daohugou area, which indicate that the Daohugou Beds were either located in the marginal regions of a lake or represent many short-lived lakes developed on the volcaniclastic apron.

3. Material and methods

3.1. Material

One hundred and sixty six spinicaudatan specimens were collected from the Yixian Formation at Jianshangou (88 specimens,

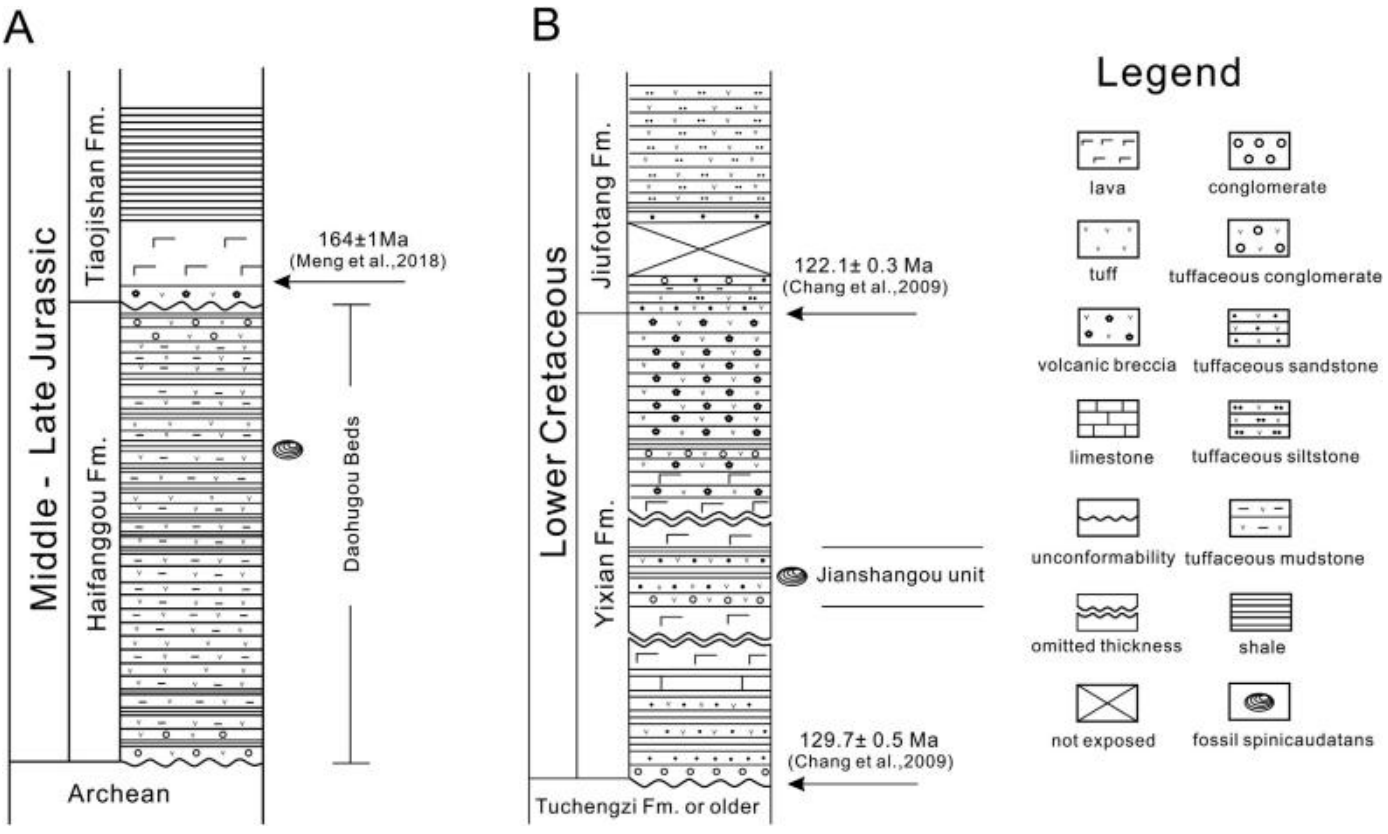

Fig. 1. Brief stratigraphic profiles of the studied sections. A, the profile of Daohugou Beds, modified from Liao et al. (2017); B, the profile of the Yixian Formation in western Liaoning, modified from Fürsich et al. (2007).

Fig. 2. Fossil spinicaudatans localities. A, map of northeastern China. B, fossil spinicaudatans localities noticed in A with red rectangle. (For interpretation of the references to colour in this figure legend, the reader is referred to the Web version of this article.)

JSG0101-JSG0429; N41°36′02.2″, E121°50′41.8″), Zhangjiagou (7 specimens, ZJG0101-ZJG0502; N41°36′13.3″, E120°49′28.7″), Erdaogou (58 specimens, EDG0101-EDG1403; N41°31′56.5″, E120°47′44.8″) and Sihetun (13 specimens; SHT0101-SHT0403, N41°36′38″, E120°49′56″) south of Beipiao, western Liaoning (Fig. 2). Most of these specimens are preserved in finely bedded tuffaceous siltstones, the rest in paper-thin laminated tuffaceous mudstones. All specimens are referable to Eosestheria (Zhang et al., 1976).

One hundred and twenty two spinicaudatan specimens were collected from the Daohugou Beds at Daohugou (98 specimens; DHG0101-DHG0806, N41°19′8″ , E119°14′13″) and Jiangzhangzi (24 specimens; JZZ0101-JZZ0704, N41°24′14″ , E119°15′40″) near Ningcheng, Inner Mongolia (Fig. 2). All specimens are preserved in tuffaceous mudstones or siltstones, which exhibit poor lamination (Shen et al., 2003). All specimens are referable to Triglypta (Liao et al., 2017).

The modern spinicaudatans Eocyzicus nanchangensis and Leptestheria sp. (referable to the same suborder Spinicaudata as the fossils) were donated by Dr. Sun Xiaoyan (from Nanjing Institute of Geology and Palaeontology, CAS), which were collected from Jiangxi Province. The specimens of Eocyzicus nanchangensis were stored in 100% ethanol until we took them out for this study. The specimens of Leptestheria sp. were stored in 65% ethanol in the field, and then dried in the stove and stored at room temperature in a clean Eppendorf tube.

The material has been deposited in the Nanjing Institute of Geology and Palaeontology, Chinese Academy of Sciences (JSG0101-JSG0429, ZJG0101-ZJG0502, EDG0101-EDG1403, SHT0101-SHT0403, DHG0101-DHG0806, JZZ0101-JZZ0704).

3.2. Methods

Based on colors of the carapaces and characteristics of the host rocks, the studied material has been categorized into eight types: five types from the Yixian Formation and three types from the Daohugou Beds (Table 1, Fig. 3).

Further analysis was based on this categorization. The selected specimens on bedding planes (at least one specimen of each type), uncoated, were mapped by energy-dispersive X-ray spectrometer (EDS, INCA 200, equipped in SEM Leo 1530VP) for elemental distribution. Afterwards, they (three specimens of type 1; one specimen of type 2; three specimens of type 3; two specimens of type 4; two specimens of type 5; two specimens of type 6; one specimen of type 7; two specimens of type 8) were coated with gold for observations under the SEM, because the charging effects of the fossil specimens were so serious. Under the SEM, EDS point analyses were performed for elemental compositions. For a closer view of the carapace microstructures, spinicaudatan specimens, still covered by sediment (three specimens of type 1; two specimens of type 6), were selected to make cross-sections after embedding them in resin; subsequently, SEM and EDS analyses were performed on the cross-sections.

All SEM and combined EDS analyses were carried out with LEO 1530VP in the Nanjing Institute of Geology and Palaeontology, Chinese Academy of Sciences. The EDS results were acquired under an acceleration voltage of 20 KeV, and at a working distance of 10 mm. The exposure time was 30 s and 30 min for spot spectrum and mapping, respectively.

Table 1
Eight spinicaudatan types based on colors of the carapaces and characteristics of host rocks.

Type	Colors of the fossils	Characteristics of host rocks	localities	Taxon	stratigraphy
1	light brown	Yellowish grey tuffaceous siltstone	Erdaogou, Sihetun, Zhangjigou	Eosestheria	Yixian Formation
2	light brown	Grey-whitish paper-thin laminated tuffaceous shale	Sihetun		
3	yellow	Yellow tuffaceous siltstone	Jianshangou, Zhangjiagou		
4	black	Yellow tuffaceous siltstone	Jianshangou, Zhangjiagou		
5	white	Yellow tuffaceous siltstone	Jianshangou		
6	dark brown	Grey tuffaceous mudstone	Daohugou	Triglypta	Daohugou Beds
7	brown	Grey tuffaceous mudstone	Jiangzhangzi		
8	no carapace	Grey-white tuffaceous mudstone	Daohugou, Jiangzhangzi		

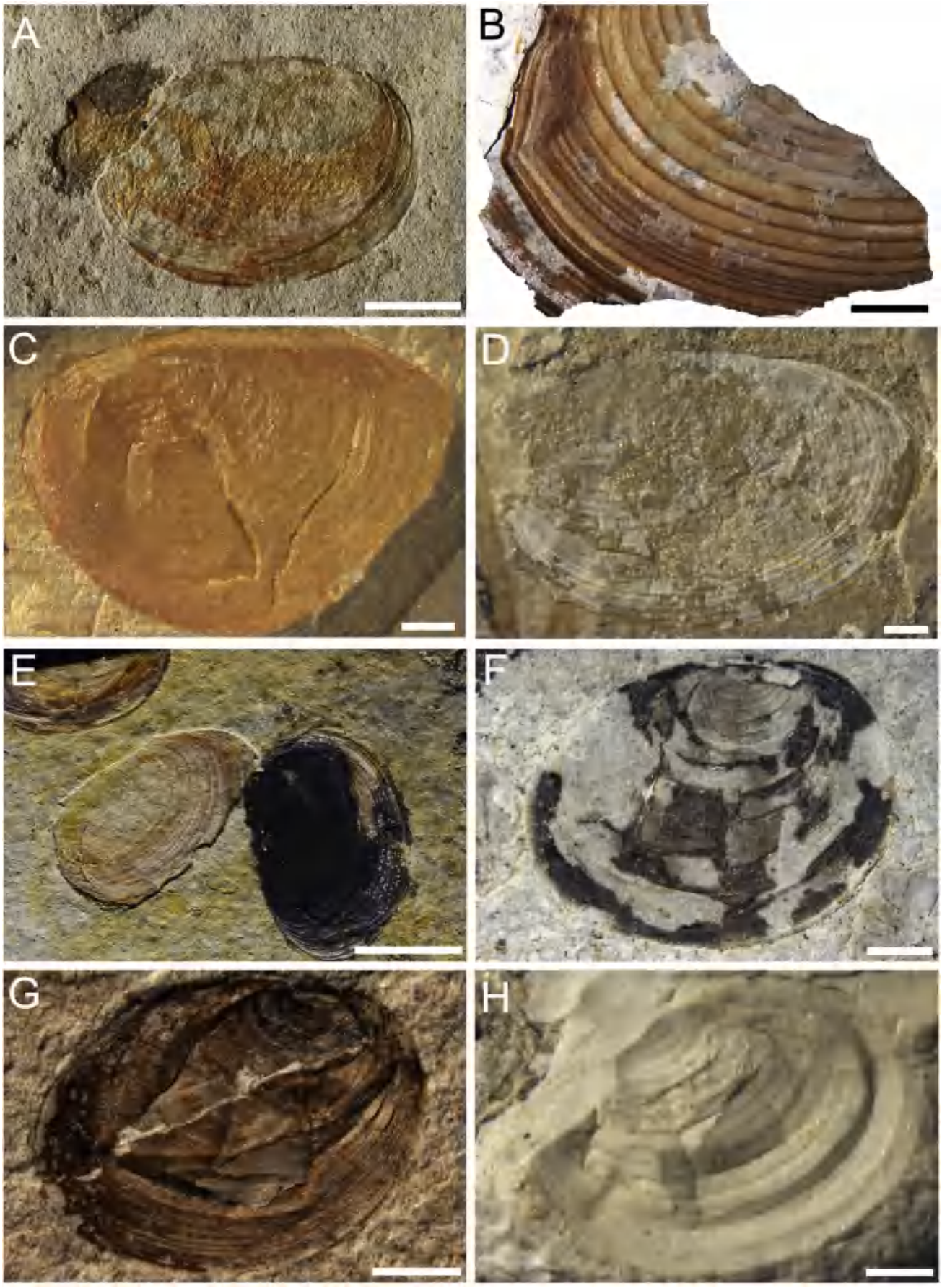
A
B
C
D
E
F
G
H

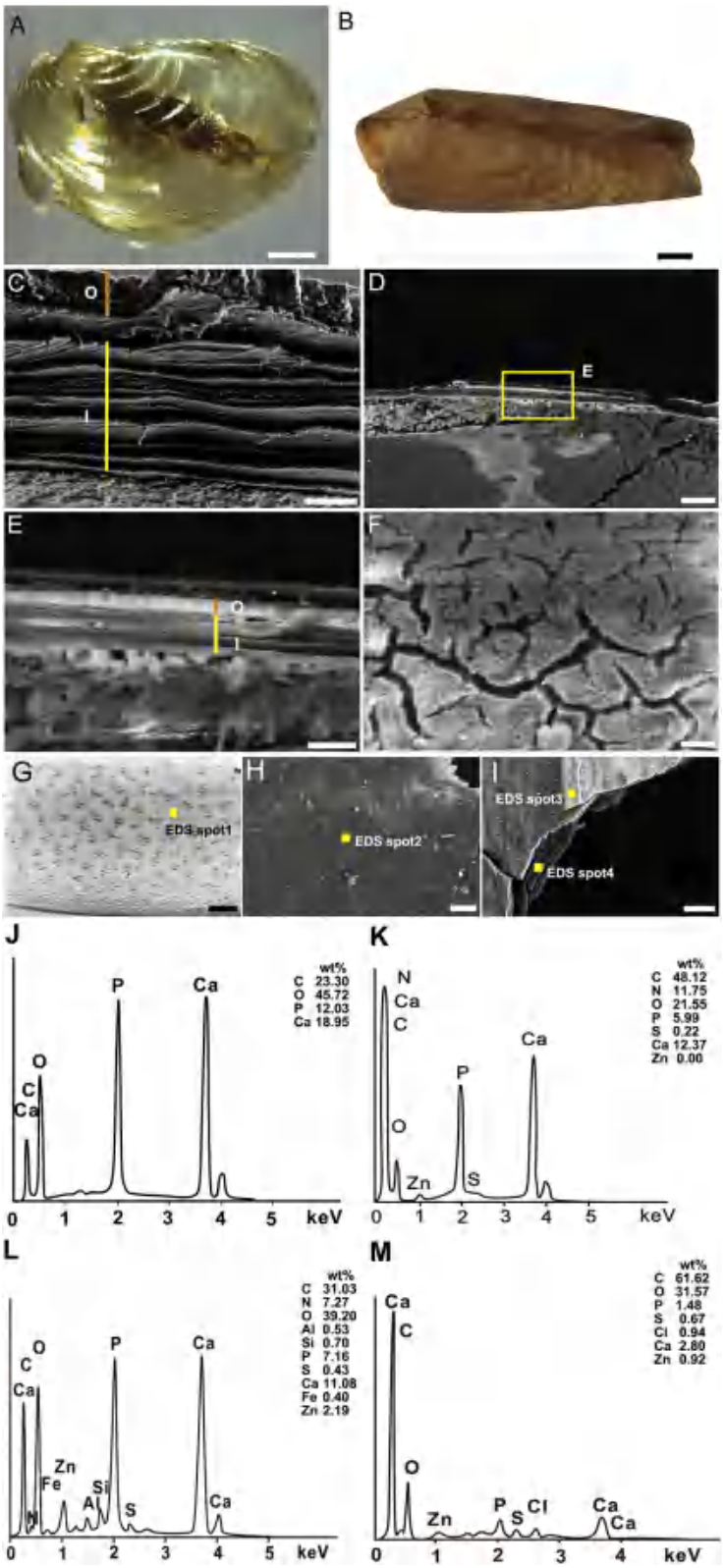

Fig. 4. Microstructure and chemical characteristics of carapaces of extant spinicaudatans. A, C, GeH, carapaces of Eocyzicus nanchangensis. B, DeF, I, carapaces of Leptestheria sp. AeB, binocular microscope images. CeE, micro-features seen in cross-sections, E is the enlarged detail from D; F, H, inner surface of the carapaces; G, I, outer surface of the carapaces. JeM, spectra of EDS spots 1e4 in G-I; C, coated with gold, under secondary electron (SE) mode; DeI, uncoated, under backscattered electron (BSE) mode. O: outer layer; I: inner layer. Scale bar = 1 mm in A-B, 50 mm in D, G, I, 20 mm in F, H, 15 mm in E, 2 mm in C.

Fig. 3. The eight types of fossil spinicaudatans based on colors of the carapaces and characteristics of host rocks. AeE, Representatives of types 1e5 from the Yixian Formation; FeH, Representatives of types 6e8 from the Daohugou Beds. Scale bar = 5 mm in A, 2 mm in B, 1 mm in C-D, FeH, 10 mm in E.

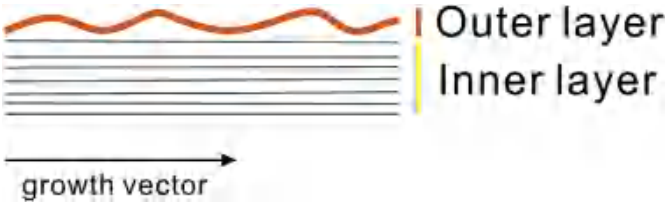

Fig. 5. Sketch of the retained outer spinicaudatan carapace after each molt in cross-section.

4. Results

4.1. Microstructure and chemical characteristics of carapaces of living spinicaudatans

Astrop (2014) showed that modern spinicaudatan carapaces in stained sections consist of epicuticle, procuticle, epidermis (contains haemocoel), inner epidermis, inner epicuticle and inner procuticle. As in most branchiopods, spinicaudatans are subject to ecdysis. Interestingly, different from most branchiopods,

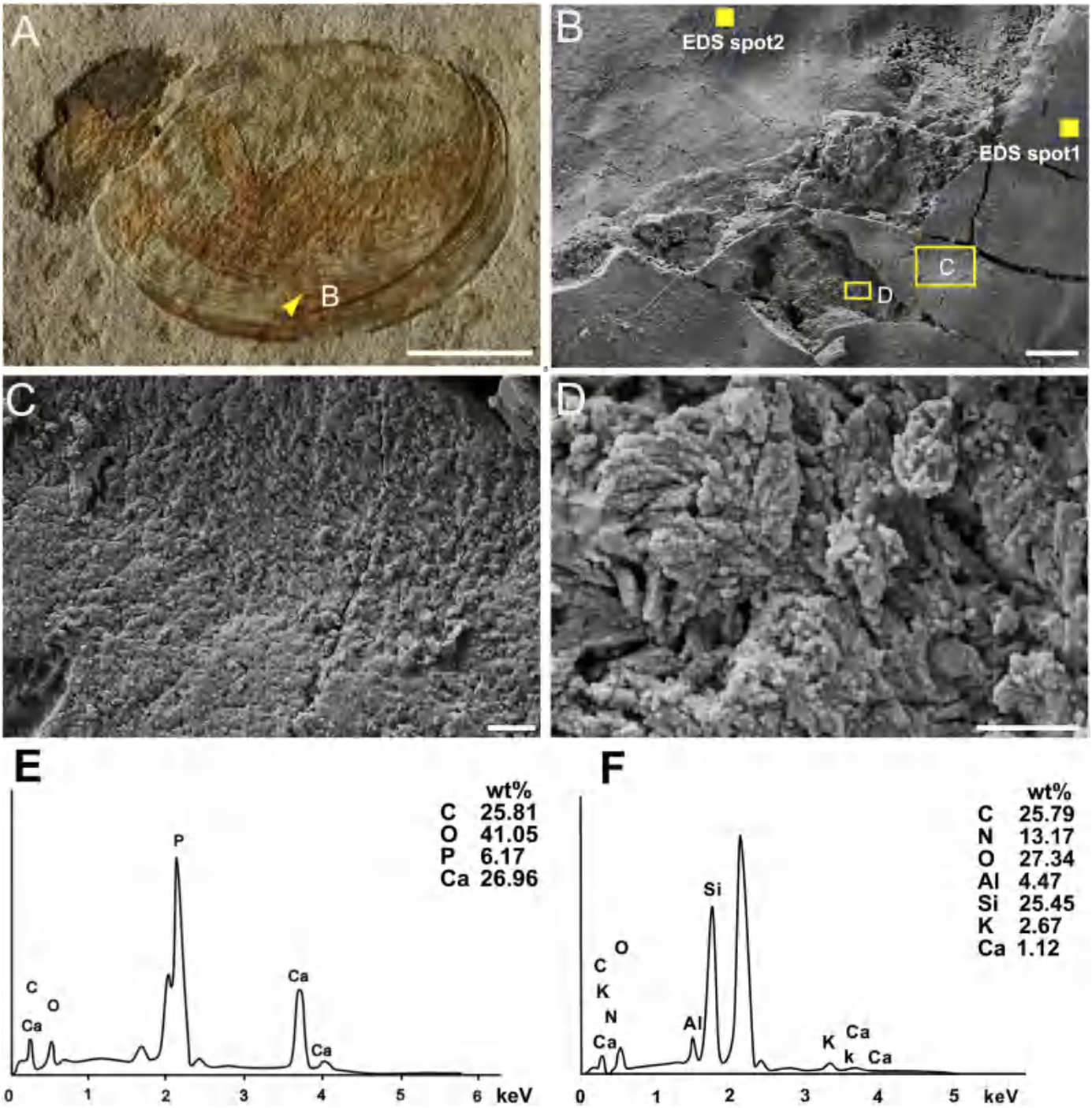

Fig. 6. Plan-view of Eosestheria sp. (Type 1, EDG0201) from the Yixian Formation. A, binocular microscope image. BeD, SEM images of the carapace, from the outside to inside; CeD, enlarged from B, C is the outer surface of the carapace; D is the inner layer of the carapace. EeF, EDS spectrum of spot 1e2 in B. B-D, coated with gold, under secondary electron (SE) mode. Scale bar = 50 mm in A, 20 ㎜ in B, 2 ㎜ in C-D.

spinicaudatans partially retain the cuticle during ecdysis. The retained cuticle consists of the epicuticle and procuticle, and a new, larger carapace nests underneath including a new epicuticle and procuticle [which is comparable to the inner epicuticle and inner procuticle (Astrop, 2014)]. The procuticle, similar to that of other branchiopods, is partly mineralized (Olempska, 2004; Astrop, 2014). As the epicuticle is very thin and easily decays even in the modern specimens, we only document the outer surface of the procuticle (Fig. 4G); thus, only the mineralized part and the chitinous part of modern carapaces are recognized under the SEM. Therefore, we designate the mineralized part of the carapace as "outer layer" and the chitinous part, which is internal to the mineralized part, as "inner layer" (Fig. 5). This designation is used only in this work to describe both the fossil carapaces and those of the living forms in the same way.

The carapaces of the modern relatives Eocyzicus nanchangensi (Fig. 4A) and Leptestheria sp. (Fig. 4B) are composed of an outer layer and an inner layer (Fig. 4C-E). Based on the backscattered z-contrast (atomic number contrast), the outer layer generally contains a higher number of atoms, which is assumed to be the mineralized layer, whereas the inner layer contains fewer atoms, which is assumed to be the chitinous layer (Fig. 4D-E, G). At higher magnification, the inner layer consists of a couple of chitinous laminae parallel to the surface (Fig. 4C, E). Additionally, the inner layer of the dehydrated carapace is full of cracks (Fig. 4F).

EDS spot analysis on the outer layer suggests that the elemental composition of this layer was mainly phosphorus (P), and calcium (Ca), with a small amount of zinc (Zn) and sulphur (S) (Fig. 4G, I, J, L; EDS spot 1, 3), and the EDS spot analysis of the inner layer shows a clear signal and higher concentration of carbon (C), but much weaker signals and lower concentration of P and Ca (Fig. 4H, I, K, M; EDS spot 2, 4). The calcium phosphate composition of our modern samples are consistent with the results found in other living forms (Stigall et al., 2008; Astrop et al., 2015).

4.2. Microstructure and chemical characteristics of Eosestheria carapaces from the Yixian Formation

In specimens preserved on bedding planes, there are usually two layers differing in the size and patterns of the crystals. We assume that the layer with small and densely packed crystals corresponds to the outer layer (Fig. 6C), and the layer with crystal aggregates and loosely distributed crystals corresponds to the inner layer (Fig. 6D). However, the EDS spot analysis and elemental mapping reveal an identical elemental composition of both layers of the Eosestheria carapaces, mainly P and Ca (Fig. 6E, EDS spot 1), differing from the rock matrix (Fig. 6F, EDS spot 2).

Here, a specimen of Type 1 (EDG0201) is shown as an example, but carapaces of other types from the Yixian Formation display a similar two-layered structure and elemental composition, except for Type 5 (see Appendix files, A.1, B.1). Specimens of Type 5 (ZJG0602) differ from the other four types from the Yixian Formation by showing local manganese (Mn) concentrations on the carapace (Fig. 7H).

In cross-section, the microstructure of Eosestheria carapaces is either almost homogeneous i.e., the outer and the inner layer cannot be distinguished or the two layers can be identified.

In the case of the former (Fig. 8A-B), the crystals of the whole carapace are small and densely packed, showing no layering. The outward-directed humps representing the growth lines are well preserved (Fig. 8B). The thickness of the valve reaches up to 60 microns (Fig. 8B).

In cases where the outer and inner layers can be recognized (Fig. 8C-D), the crystals of the outer layer are small and densely packed (indicated by "O" in Fig. 8D), but those of the inner layer are loosely distributed (indicated by "I" in Fig. 8D). This is identical to what is observed on the specimens on bedding planes. The undulations on the outer layer, which represent the external shell ornamentation of the growth bands, such as reticulations or punctae, are well preserved (Fig. 8D). Besides, the inner layer shows laminae parallel to the surface ("I" in Fig. 8D), which are similar to the original chitinous laminae. The valve thickness is about 22 microns (Fig. 8D).

The EDS point analysis of the carapace shows peaks of P and Ca (Fig. 8E-F, EDS spots 1e2), the same as the results obtained from the specimens on bedding planes. Additionally, the resin may contribute to the C peak, as seen in the C map of the cross-section that shows C is more concentrated where space between host rock and fossils is filled with resin (Fig. 8H, C map).

All examined Eosestheria carapaces from the Yixian Formation display a uniform elemental composition, which is mainly P and Ca. It seems that the complete carapaces have been phosphatized in addition to the original biomineralized outer layer.

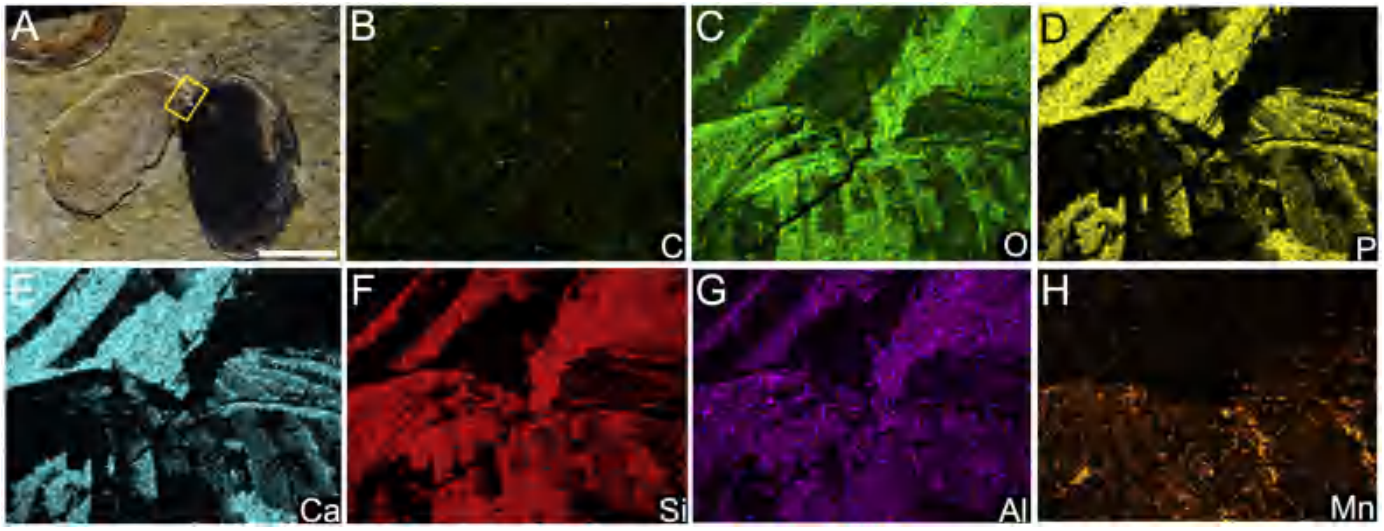

Fig. 7. Elemental mapping of Eosestheria sp. from the Yixian Formation (Type 5, ZJG0602). A, Binocular microscope image. BeH, EDS maps of Carbon (C), Oxygen (O), Phosphorus (P), Calcium (Ca), Silicon (Si), Aluminum (Al), and Manganese (Mn). The area of elemental mapping is within the yellow box in A. Color intensity corresponds to relative elemental abundance. Scale bar = 1 cm. (For interpretation of the references to colour in this figure legend, the reader is referred to the Web version of this article.)

4.3. Microstructure and chemical characteristics of Triglypta carapaces from the Daohugou Beds

In specimens preserved on bedding planes, two layers can be recognized. The outer layer is composed of small, compact crystals (Fig. 9C) and exhibits punctae on the surface (Fig. 9B), while the inner layer is full of cracks (Fig. 9B, F). The inner surface layer (enlarged detail, Fig. 8D) is smoother than the surface of the outer layer (Fig. 9C).

EDS spot 2 of the inner layer of a Type 6 carapace showed weaker signals and lower concentration of P and Ca (Fig. 9D, H, EDS spot2) but stronger signal and higher concentration of C than those of the outer layer (Fig. 9B, G, EDS spot 1), which is comparable to the outer and inner layers of the modern carapaces (Fig. 4). EDS mapping on the bedding plane (Type 6, DHG0501) suggests the C is concentrated (Fig. 10B, C map), which confirmed the EDS spot analysis. The EDS analysis of Type 7 of the outer layer also shows clear peaks of P and Ca (Fig. 9F, I, EDS spot 3), similar to the outer

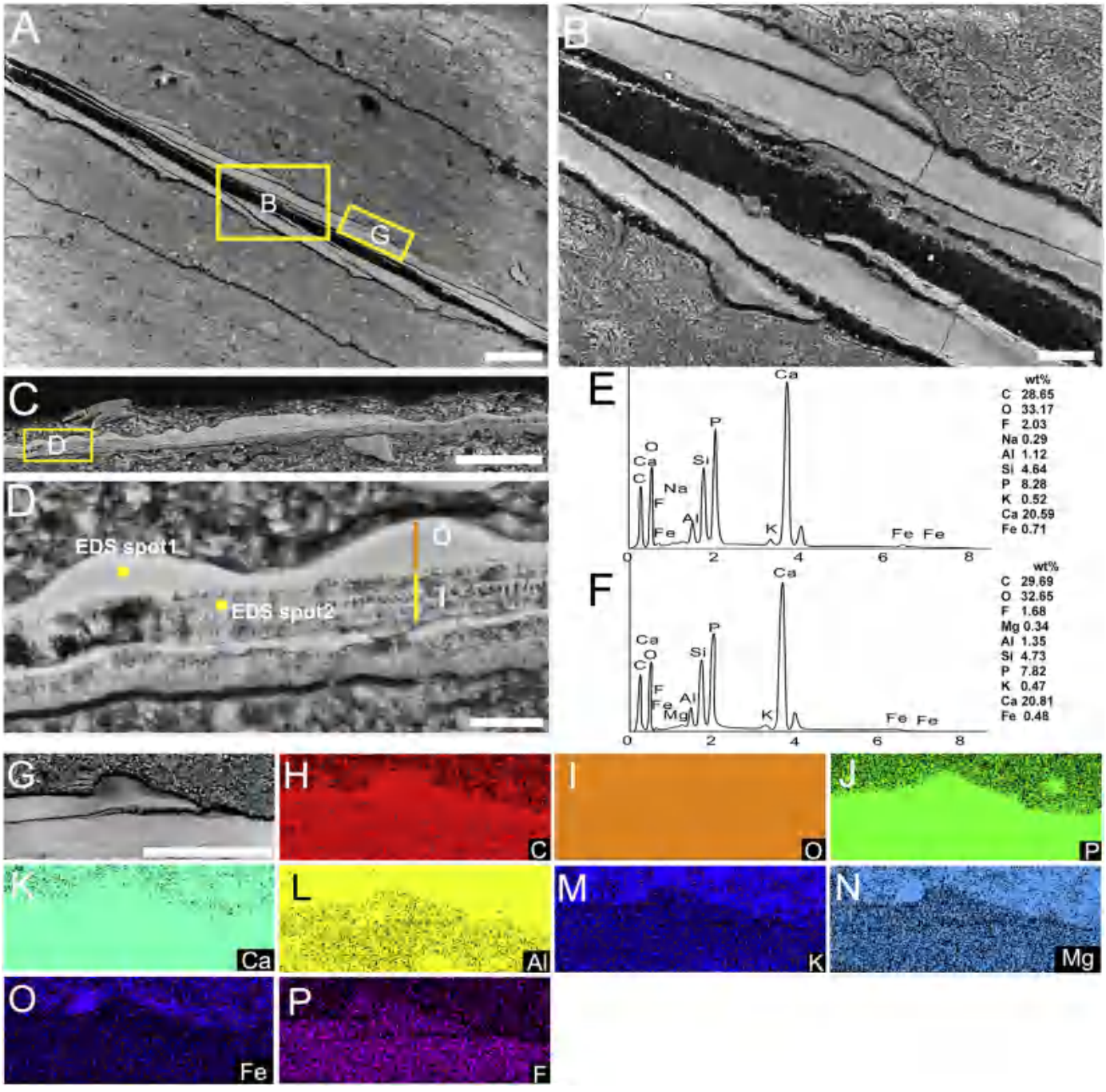

Fig. 8. SEM images of transverse cross-sections of Eosestheria sp. from the Yixian Formation (Type 1). A-B, Specimen from Zhangjiagou (ZJG06), B is enlarged from A, showing the homogeneously permineralized carapace; C-D, Specimen from Sihetun (SHT05), D is enlarged from C, showing identifiable outer layer (orange line) and inner layer (yellow line). E-F, EDS spectra of spots 1e2 in D. G, Area of elemental mapping from A; HeP, maps of C, O, P, Ca, Al, K, Mg, Fe, and F. A-D, G, uncoated, under backscattered electron (BSE) mode. O: outer layer; I: inner layer. Scale bar = 200 mm in A, 40 mm in B, 100 mm in C, G, 10 mm in D. (For interpretation of the references to colour in this figure legend, the reader is referred to the Web version of this article.)

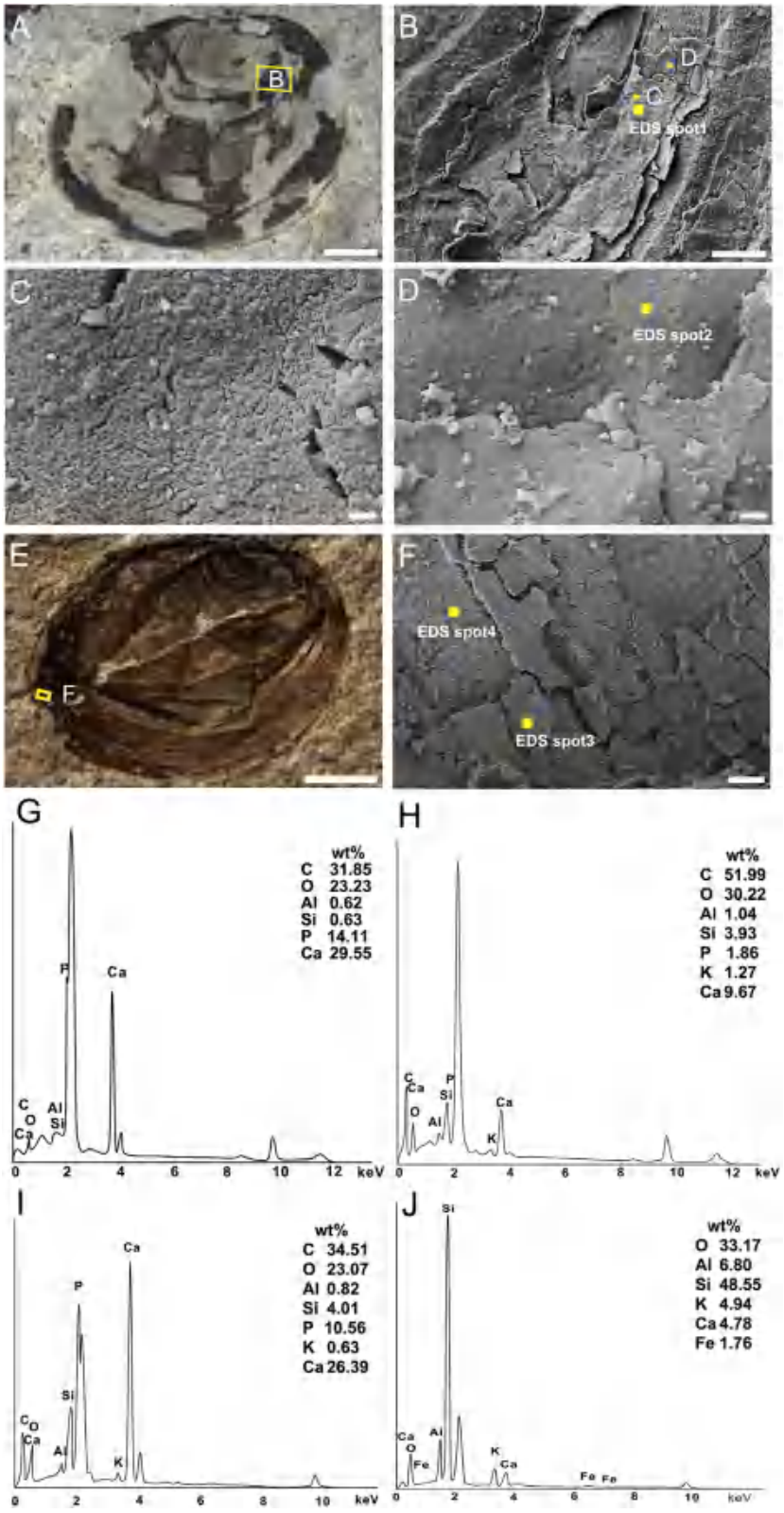

Fig. 9. Bedding plane view of Triglypta sp. from the Daohugou Beds (A-D, Type 6, DHG0401; E-F, Type 7, JZZ0301). A, E, binocular microscope image. B-D, SEM images of the carapace, from outside to inside, C is the outer surface of the carapace enlarged from B, C is the inner layer of the carapace enlarged from B. F, outer surface of the carapace enlarged from E. G-J, EDS spectra of spots 1e4 in B, D, and F, respectively. B-D, F, coated with gold, under secondary electron (SE) mode. Scale bar = 1 mm in A, E, 100 ㎜ in B, 1 ㎜ in C-D, 20 ㎜ in F.

layer of the modern carapaces (Fig. 4J, L, EDS spot 1, 3). The element components of the rock matrix are mainly aluminosilicate (Fig. 9F, J, EDS spot4).

In the specimens of Type 8 (DHG0801, an external mould), no microstructure of carapaces are identified. It is hard to say whether they are different or identical to other types. The results are shown in Appendix files A.2 and B.2.2.

In cross-sections, the outer and inner layers can be distinguished based on the backscattered z-contrast (atomic number contrast) (Fig. 11A). Associated with the EDS mapping analysis, the outer layer is mainly composed of P and Ca (Fig. 11F-G), while the inner layer shows local concentrations of C (Fig. 10E). The valve thickness is less than 10 microns (Fig. 11A), which is much less than in the specimens from the Yixian Formation.

The compact structure, relatively low contrast in the backscattered mode and cracks of the inner layer, combined with the EDS point and mapping analysis suggest that the inner layer of the spinicaudatan carapaces from the Daohugou Beds contains carbonaceous remains, which are absent in the carapaces from the Yixian Formation.

5. Discussion

5.1. Comparison of the microstructure of fossil and modern spinicaudatan carapaces

Spinicaudatans are commonly preserved as bivalved carapaces in non-marine deposits. The ornamentation of the carapace surface is a critical feature to distinguish fossil taxa (Zhang et al., 1976; Chen, 1999; Li et al., 2017). However, the microstructure of fossil spinicaudatan carapaces is poorly known. Olempska, (2004) figured the multilayer structure of Triassic spinicaudatan carapaces from Poland, and suggested that the fossil carapaces consist of an ornament-bearing outer layer and a chitinous inner layer.

The Eosestheria carapaces from the Yixian Formation of our study are permineralized, with no signs of organic material left. Usually two layers can be identified: an outer layer and an inner layer. The laminae in the inner layer are similar to the laminae in living spinicaudatan carapaces. Besides, the amorphous fibre-like structures are also morphologically similar to the chitin fibrils in the cuticles of living forms, which consist of long-chain polysaccharide chitin. These fibrils are assembled into bundles, making up the laminae parallel to the surface (Feng, 2011). Thus, the inner layer of the fossil carapace is comparable to the chitinous layer, while the outer layer corresponds to the mineralized part of the procuticle.

Based on the high concentration of phosphate and calcium of inner layers, phosphatization is most likely the principal diagenetic process of the fossil carapaces, though the presence of low concentration of Al, K, Si, which probably indicating the partly silification of some carapaces. The possible other diagenetic processes are left to determine later after this work.

In specimens preserving the amorphous fibre-like structure, phosphatization probably occurred before thorough decay, replaced the chemical constituents and preserved the fibre-like structure. In rare cases, the fossil carapace is uniformly composed of small and densely packed crystals, showing no layering. There, phophatization either occurred later or recrystallization took place.

The carapaces of Triglypta from the Daohugou Beds also contain two layers. The outer layer contains relatively higher concentrations of P and Ca, which is comparable to the elements composition of the biomineralized outer layer of the modern carapaces. While the inner layer showed a strong signal and high concentration of C and much weaker signals and lower concentrations of P and Ca, compared to the outer layer. Such an element composition is comparable to that of the inner layer of the modern carapace. The cracks occurred in the inner layer of Triglypta, such features are also occurred in the chitinous inner layer of dehydrated modern carapaces. Thus, we assumed that the outer and inner layers of Triglypta were comparable to the outer and the inner layers of living relatives, and the inner layer of Triglypta can be correlated to the chitinous layer of the modern carapaces. Chitin is one of the basic material to form the exoskeletons of arthropods (Fabritius et al., 2011). However, chitin easily changes into an aliphatic composition during long-term diagenesis (Briggs, 1999; Gupta et al., 2007). Such stable aliphatic composition can be formed by in-situ transformation without high temperatures or pressure (Briggs et al., 2000). Most likely, the carbonaceous remains of carapaces from the Daohugou Beds are no longer the original chitin fibrils, but aliphatic biopolymers. This is also the reason why no fibre-like structures are observed in the inner layer of carapaces from the Daohugou Beds. However, the exact composition remains to be determined. Despite the preservation of carbonaceous material from the Daohugou Beds, the laminae of modern spinicaudatan carapaces are no longer recognizable in these specimens, which may be due to compaction during diagenesis.

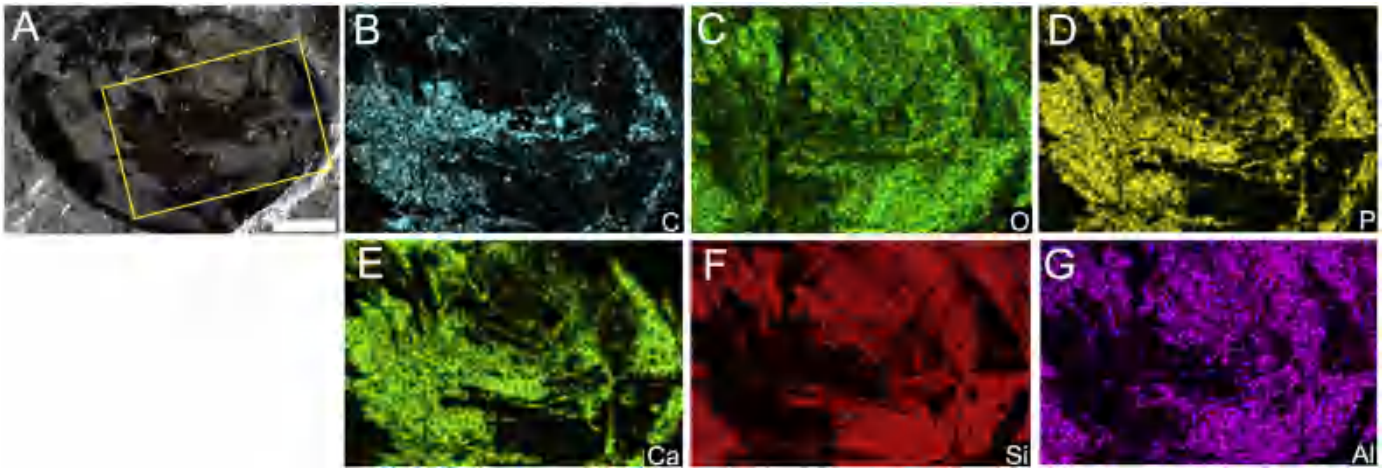

Fig. 10. Elemental mapping of Triglypta sp. from the Daohugou Beds (type 6, DHG05-1). A, binocular microscope image, the yellow rectangle indicates the area of elemental mapping; BeG, maps of C, O, P, Ca, Si, and Al. Scale bar = 1 mm in A. (For interpretation of the references to colour in this figure legend, the reader is referred to the Web version of this article.)

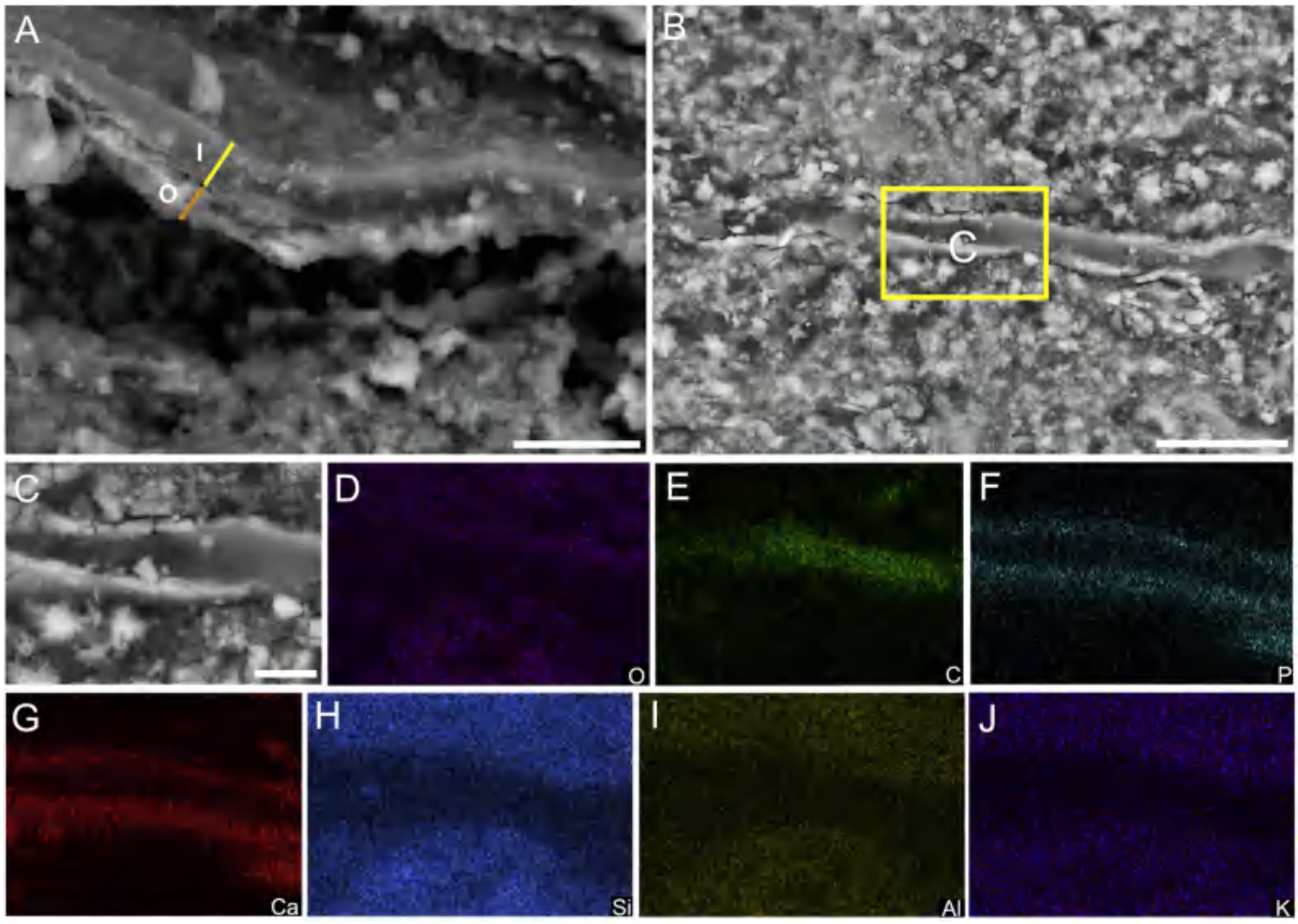

Fig. 11. Cross-sections of Triglypta sp. from the Daohugou Beds (type 6, DHG05). A, Single valve, showing the outer layer (orange line) and the inner layer (yellow line); B–C, cross-section of an articulated specimen, C is the enlarged area from B for elemental mapping. D-J, maps of O, C, P, Ca, Si, Al, and K. A-C, uncoated, under backscattered electron (BSE) mode. O: outer layer; I: inner layer. Scale bar = 20 μm in B, 10 μm in A, 5 μm in C. (For interpretation of the references to colour in this figure legend, the reader is referred to the Web version of this article.)

5.2. Phosphatization of Eosestheria carapaces from the Yixian Formation

Phosphatization is one of the most important taphonomic pathways to exceptional preservation (Briggs et al., 1993; Dornbos, 2011). Phosphate is an important biomineralization component of the spinicaudatan carapaces (Vannier et al., 2003; Stigall and Hartman, 2008; Astrop, 2014). As no phosphorus signals were detected in the rock matrix of our samples, the carapaces themselves might have been the source of phosphorous during mineralization in both cases. An alkaline microenvironment can promote phosphate precipitation (Berner, 1968; Gulbrandsen, 1969; Allison, 1988). However, usually the decay of the carcass decreases the pH of the microenvironment (Klug et al., 2005), and very acidic conditions would inhibit the precipitation of phosphate (Gabbott, 1998; Briggs, 2003). In the case of the paleo-lakes of the Yixian Formation and the Daohugou Beds, frequent volcanic ash input and decomposition of the volcanic glass particles contributed to the alkalinity of water, but the decay of organisms and the emission of CO_2 by volcanic processes may have increased the acidity, which most likely led to fluctuations of the alkalinity and acidity of these lake water (Fürsich and Pan, 2015). The lake of the Yixian Formation presumably was more alkaline so that the decrease of the pH due to decay processes was not sufficient to inhibit phosphatization. In contrast, in the case of the Daohugou Beds the lake waters could not neutralize the decrease in pH of the microenvironment in the vicinity of the decaying carcasses, so that phosphatization has been inhibited to some extent.

5.3. Carbonaceous remains in invertebrate cuticles from the Yanliao Biota but not from the Jehol Biota

Our studies found carbonaceous remains preserved in Yanliao, but not in Jehol spinicaudatan carapaces, which is consistent with previous studies. Wang et al. (2008) suggested that most of the fossil insects from the Daohugou Beds are preserved organic remains as carbonaceous compressions, and only some of them are pyritized. Fürsich and Pan (2015), by comparing the bivalves from the Daohugou Beds and the Yixian Formation, suggested that the Jurassic bivalves contain remains of the organic periostracum, while the Lower Cretaceous bivalves preserve no carbonaceous remains. Apparently, the paleo-lake of the Yanliao Biota had a higher potential to preserve carbonaceous remains of the invertebrates, such as diagenetic products of cuticles.

5.4. Comparison of the eight spinicaudatan types

The rock matrix of the fossils from the Yixian Formation and Daohugou Beds differs. The former consists mainly of tuffaceous siltstones, except for type 2, the latter of tuffaceous mudstones. Our

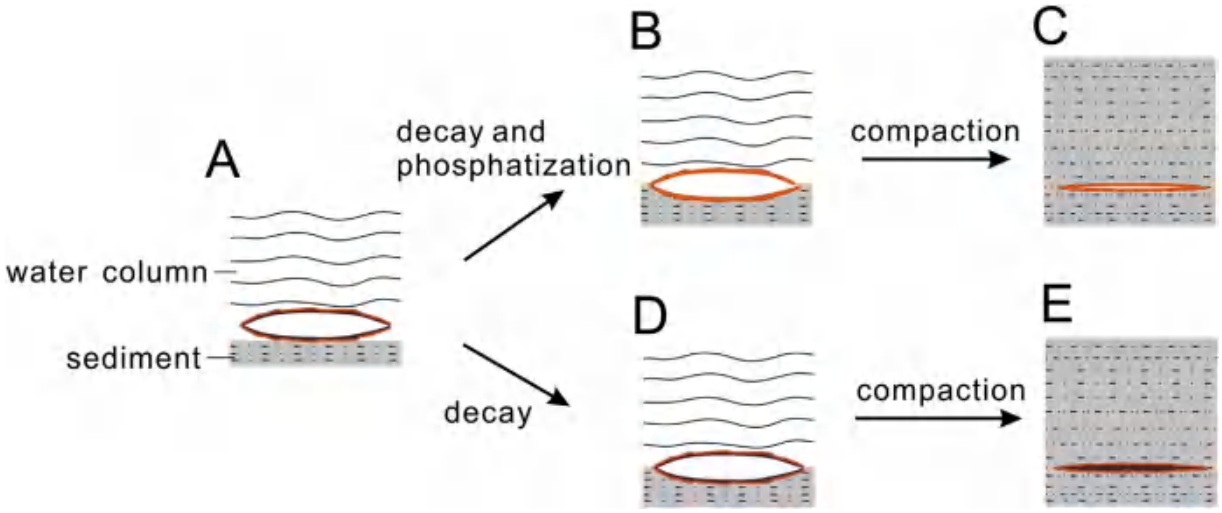

Fig. 12. Diagenetic pathways of spinicaudatans from the Yixian Formation (AeC) and the Daohugou Beds (A, DeE).

analysis suggests that for all types from the Yixian Formation preservational conditions were similar, but differed from those of the types from the Daohugou Beds. Therefore the different rock types may have influenced the preservation of the spinicaudatan carapaces. The precise mineral compositions of rock matrices need to be checked to confirm this deduction.

Color differences were the main characteristics for the type classification. The spinicaudatan carapaces from the Yixian Formation are preserved as light brown, yellow, black, or white remains, whereas those from the Daohugou Beds are preserved as dark brown and brown remains, occasionally as external moulds with small fragments of carapaces material (Type 8). Tasch (1982) associated the color of carapaces with the temperature during diagenesis. Heating experiments on modern spinicaudatan valves show that glossy black colors appear at 300°e400°, a light-brown crust appears at 450°e600°, white color appears at 600°e1100°, white enameloid plus brown crust appears at 800°e1100°, and at 1200°, valves become transparent glassy. Such experimentally determined color classes were found in fossil carapaces from Blizzard Heights and Mauger Nunatak (Tasch, 1982). Monferran et al. (2018) also ascribed the different colors of spinicaudatan carapaces from the Cañadón Asfalto Formation to specific preservation modes. Our analysis on the microstructure of the four different colors of carapaces from the Yixian Formation show no obvious differences, and the EDS results show that the black carapaces contain abundant Manganese, while others show no evident differences. Manganese coating commonly occurs in natural deposits (Potter and Rossman, 1979), such as the manganese dendrite pseudofossils. Thus the black samples may be attributed to manganese impregnation. However, temperature could also be the reason of various colors in the specimens preserved in deposits affected by volcanic processes. Further analyses, including semi-quantitative and quantitative analysis on the chemical composition of carapaces and the mineral composition of the rock matrix, are needed to evaluate the relationship between the carapace colors and paleoenvironment factors.

5.5. Taphonomic pathways

Modern spinicaudatan carapaces are composed of a calcium-phosphate-chitin composite (Stigall et al., 2008; Astrop et al., 2015) and are resistant to numerous biological and taphonomic processes such as transport, decay, etc. to be preserved in the sediment as fossils (Astrop and Hegna, 2015). Most analyzed fossil carapaces are preserved as recrystallized calcium phosphate or silica replaced molds (Stigall and Hartman, 2008; Stigall et al., 2008, 2014; Hethke et al., 2013; Monferran et al., 2018). Carbonate preservation is relatively rare (Lucas and Milner, 2006; Stigall et al., 2017). Combining the microstructure studies with EDS analyses, our study suggests that the different layers of the carapaces may undergo separate diagenetic processes. The outer layers of the carapaces of all investigated specimens are preserved as calcium phosphate, but the inner layers of the spinicaudatans from the Yixian Formation have been phosphatized and those from the Daohugou Beds are preserved as carbonaceous material.

The general taphonomic pathways of Eosestheria from the Yixian Formation and of Triglypta from the Daohugou Beds can be reconstructed as follows (Fig. 12): In the case of Eosestheria (Fig. 12A-C), the carcasses began to decay to some extent under dysoxic-anoxic conditions after arriving on the bottom of the lake, phosphatization occurred and phosphate minerals replaced the organic material of the carapace. In the case of Triglypta (Fig. 12A, D-E), the decay and phosphatization of the carapaces probably were inhibited to some extent, so that the organic material of the carapace could be preserved. Although the EDS detected the phosphorus signals from the specimens of the Daohugou Beds, we cannot confirm at the present stage whether the carapaces experienced recrystallization or not because the minerals of the carapaces may stem from the biomineralization. However, the carbonaceous remains of the carapaces suggest that phosphatization has been inhibited to some degree. Further mineral analyses are needed to corroborate the conclusions reached here.

6. Conclusions

The carapaces of spinicaudatans from the Yixan Formation are permineralized, and partially preserve the morphological information of the original chitin fibrils. In contrast, the carapaces of spinicaudatans from the Daohugou Beds preserve organic materials, which most likely are remains of chitin, but the exact composition remains to be determined. Based on the investigation of the carapace microstructure of spinicaudatans from the Jehol and Yanliao biota, we speculate that the paleo-lake of the Yanliao Biota had a higher potential to preserve organic remains such as cuticles.

Acknowledgements

The authors benefited from discussions with Xiao Teng and Huanyu Liao. Xiaoyan Sun kindly provided us with the modern spinicaudatan specimens. We benefitted from the lab in the Key Laboratory of Unconventional Oil and Gas Geology, China Geological Survey. The study was supported by the Strategic Priority Research Program of the Chinese Academy of Sciences, Grant No. XDB26000000, the National Natural Science Foundation of China (41472009, 41688103, 41602012), Youth Innovation Promotion Association CAS to Pan Yanhong and Open-Lab Grants of the State Key Laboratory of Palaeontology and Stratigraphy, NIGPAS. We thank Prof. Franz T. Fürsich and Prof. Oscar F. Gallego for reviewing and improving the paper.

References

Allison, P.A., 1988. Phosphatized soft-bodied squids from the Jurassic Oxford Clay. Lethaia 21, 403e410.

Astrop, T.I., 2014. The evolutionary dynamics of sexual systems in deep time: an integrated biological and paleontological approach. PhD thesis. University of Akron, 233 pp.

Astrop, T.I., Hegna, T.A., 2015. Phylogenetic relationships between living and fossil spinicaudatan taxa (Branchiopoda Spinicaudata): Reconsidering the evidence. Journal of Crustacean Biology 35, 339e354.

Astrop, T.I., Sahni, V., Blackledge, T.A., Stark, A.Y., 2015. Mechanical properties of the chitin-calcium-phospate "clam shrimp" carapace (Branchiopoda: Spinicaudata): Implications for taphonomy and fossilization. Journal of Crustacean Biology 35, 123e131.

Benton, M.J., Zhou, Z.-H., Patrick, J.O., Zhang, F.-C., Stuart, L.K., 2008. The remarkable fossils from the Early Cretaceous Jehol Biota of China and how they have changed our knowledge of Mesozoic life: Presidential Address, delivered 2nd May 2008. Proceedings of the Geologists' Association 119, 209e228.

Berner, R.A., 1968. Calcium carbonate concretions formed by the decomposition of organic matter. Science 159, 195e197.

Briggs, D.E.G., 1999. Molecular taphonomy of animal and plant cuticles: selective preservation and diagenesis. Philosophical Transactions of the Royal Society of London B: Biological Sciences 354, 7e17.

Briggs, D.E.G., 2003. The role of decay and mineralization in the preservation of soft-bodied fossils. Annual Review of Earth and Planetary Sciences 31, 275e301.

Briggs, D.E.G., Evershed, R.P., Lockheart, M.J., 2000. The biomolecular paleontology of continental fossils. Paleobiology 26, 169e193.

Briggs, D.E.G., Kear, A., Martill, D., Wilby, P., 1993. Phosphatization of soft-tissue in experiments and fossils. Journal of the Geological Society 150, 1035e1038.

Chang, M.-M., Chen, P.-J., Wang, Y.-Q., Wang, Y., 2003. The Jehol Biota: The emergence of feathered dinosaurs, beaked birds and flowering plants. Shanghai Scientific and Technical Publishers, Shanghai, 208 pp.

Chang, S.-C., Gao, K.-Q., Zhou, C.-F., Jourdan, F., 2017. New chronostratigraphic constraints on the Yixian Formation with implications for the Jehol Biota. Palaeogeography, Palaeoclimatology, Palaeoecology 487, 399e406.

Chen, P.-J., 1999. Fossil conchostracans from the Yixian Formation of western Liaoning, China. Palaeoworld 11, 114e130 (in Chinese, English abstract).

Chen, W., Ji, Q., Liu, D.-Y., Zhang, Y., Song, B., Liu, X.-Y., 2004. Isotope geochronology of the fossil-bearing beds in the Daohugou area, Ningcheng, Inner Mongolia. Geological Bulletin of China 23, 1165e1169 (in Chinese, English abstract).

Dornbos, S.Q., 2011. Phosphatization through the Phanerozoic. In: Allison, P.A., Bottjer, D.J. (Eds.), Taphonomy, second ed. Springer, pp. 435e456.

Fabritius, H., Sachs, C., Raabe, D., Nikolov, S., Friák, M., Neugebauer, J., 2011. Chitin in the exoskeletons of Arthropoda: From ancient design to novel materials science. In: Gupta, N.S. (Ed.), Chitin. Springer, pp. 35e60.

Feng, Q., 2011. Principles of calcium-based biomineralization. In: Müller, W.E.G. (Ed.), Molecular Biomineralization. Springer, pp. 141e197.

Fürsich, F.T., Pan, Y.-H., 2015. Diagenesis of bivalves from Jurassic and Lower Cretaceous lacustrine deposits of northeastern China. Geological Magazine 153, 17e37.

Fürsich, F.T., Sha, J.-G., Jiang, B.-Y., Pan, Y.-H., 2007. High resolution palaeoecological and taphonomic analysis of Early Cretaceous lake biota, western Liaoning (NE-China). Palaeogeography, Palaeoclimatology, Palaeoecology 253, 434e457.

Gabbott, S.E., 1998. Taphonomy of the Ordovician Soom Shale Lagerstätte: an example of soft tissue preservation in clay minerals. Palaeontology 41, 631e668.

Grabau, A.W., 1928. Stratigraphy of China. Part 2 Mesozoic. Geological Survey of China, Beijing, 774 pp.

Gupta, N.S., Briggs, D.E.G., Collinson, M.E., Evershed, R.P., Michels, R., Jack, K.S., Pancost, R.D., 2007. Evidence for the in situ polymerisation of labile aliphatic organic compounds during the preservation of fossil leaves: implications for organic matter preservation. Organic Geochemistry 38, 499e522.

Gu, Z.-W., 1962. Jurassic and Cretaceous of China. Science Press, Beijing, 84 pp (in Chinese).

Gulbrandsen, R., 1969. Physical and chemical factors in the formation of marine apatite. Economic Geology 64, 365e382.

Hethke, M., Fürsich, F.T., Jiang, B.-Y., Pan, Y.-H., 2013. Seasonal to sub-seasonal palaeoenvironmental changes in Lake Sihetun (Lower Cretaceous Yixian Formation, NE China). International Journal of Earth Sciences 102, 351e378.

Huang, D.-Y., 2015. Yanliao biota and Yanshan movement. Acta Palaeontologica Sinica 54, 501e546 (in Chinese, English abstract).

Huang, D.-Y., 2016. The Daohugou Biota. Shanghai Scientific and Technical Publishers, Shanghai, 336 pp (in Chinese, English abstract).

Huang, D.-Y., Cai, C.-Y., Jiang, J.-Q., Su, Y.-T., Liao, H.-Y., 2015. Daohugou bed and fossil record of its basal conglomerate section. Acta Palaeontologica Sinica 54, 351e357 (in Chinese, English abstract).

Jiang, B.-Y., Sha, J.-G., 2007. Preliminary analysis of the depositional environments of the Lower Cretaceous Yixian Formation in the Sihetun area, western Liaoning, China. Cretaceous Research 28, 183e193.

Jiang, B.-Y., Fürsich, F.T., Sha, J.-G., Wang, B., Niu, Y.-Z., 2011. Early Cretaceous volcanism and its impact on fossil preservation in Western Liaoning, NE China. Palaeogeography, Palaeoclimatology, Palaeoecology 302, 255e269.

Jiang, B.-Y., Fürsich, F.T., Hethke, M., 2012. Depositional evolution of the Early Cretaceous Sihetun Lake and implications for regional climatic and volcanic history in western Liaoning, NE China. Sedimentary Geology 257e260, 31e44.

Jiang, B.-Y., Harlow, G.E., Wohletz, K., Zhou, Z.-H., Meng, J., 2014. New evidence suggests pyroclastic flows are responsible for the remarkable preservation of the Jehol biota. Nature Communications 5, 3151.

Klug, C., Hagdorn, H., Montenari, M., 2005. Phosphatized soft-tissue in Triassic bivalves. Palaeontology 48, 833e852.

Leng, Q., Yang, H., 2003. Pyrite framboids associated with the Mesozoic Jehol Biota in northeastern China: Implications for microenvironment during early fossilization. Progress in Natural Science 13, 206e212.

Li, G., Boukhalfa, K., Teng, X., Soussi, M., Ali, W.B., Ouaja, M., Houla, Y., 2017. New Early Cretaceous clam shrimps (Spinicaudata) from uppermost Bouhedma Formation of northern Chotts range, southern Tunisia: Taxonomy, stratigraphy and palaeoenvironmental implications. Cretaceous Research 72, 124e133.

Liao, H.-Y., Shen, Y.-B., Huang, D.-Y., 2017. Conchostracans of the MiddleeLate Jurassic Daohugou and Linglongta beds in NE China. Palaeoworld 26, 317e330.

Liu, Y.-Q., Liu, Y.-X., Ji, S.-A., Yang, Z.-Q., 2006. SHRIMP U-Pb zircon age for the Daohugou Biota at Ningcheng of Inner Mongolia and comments on related issues. Chinese Science Bulletin 51, 2273e2282 (in Chinese).

Lucas, S.G., Milner, A.R.C., 2006. Conchostraca from the Lower Jurassic Whitmore Point Member of the Moenave Formation, Johnson Farm, Southwestern Utah. In: Harris, J.D., Lucas, S.G., Spielmann, J.A., Lockley, M.G., Milner, A.R.C., Kirkland, J.I. (Eds.), The Triassic-Jurassic Terrestrial Transition. New Mexico Museum of Natural History and Science, vol. 37. Bulletin, Albuquerque, pp. 421e423.

Meng, F.-X., Gao, S., Song, Z.-J., Niu, Y.-L., Li, X.-P., 2018. Mesozoic high-Mg andesites from the Daohugou area, Inner Mongolia: Upper-crustal fractional crystallization of parental melt derived from metasomatized lithospheric mantle wedge. Lithos 302, 535e548.

Monferran, M.D., D'Angelo, J.A., Cabaleri, N.G., Gallego, O.F., Garban, G., 2018. Chemical taphonomy and preservation modes of Jurassic spinicaudatans from Patagonia: a chemometric approach. Journal of Paleontology 92, 1e12.

Olempska, E., 2004. Late Triassic spinicaudatan crustaceans from southwestern Poland. Acta Palaeontologica Polonica 49, 429e442.

Pan, Y.-H., Sha, J.-G., Fürsich, F.T., 2014. A model for organic fossilization of the Early Cretaceous Jehol Lagerstätte based on the taphonomy of "Ephemeropsis trisetalis". PALAIOS 29, 363e377.

Pan, Y.-H., Sha, J.-G., Fürsich, F.T., Wang, Y.-Q., Zhang, X.-L., Yao, X.-G., 2012. Dynamics of the lacustrine fauna from the Early Cretaceous Yixian Formation, China: implications of volcanic and climatic factors. Lethaia 45, 299e314.

Pan, Y.-H., Sha, J.-G., Zhou, Z.-H., Fürsich, F.T., 2013. The Jehol Biota: Definition and distribution of exceptionally preserved relicts of a continental Early Cretaceous ecosystem. Cretaceous Research 44, 30e38.

Potter, R.M., Rossman, G.R., 1979. Mineralogy of manganese dendrites and coatings. American Mineralogist 64, 1219e1226.

Ren, D., Gao, K.-Q., Guo, Z.-G., Ji, S.-A., Tan, J.-J., Song, Z., 2002. Stratigraphic division of the Jurassic in the Daohugou area, Ningcheng, Inner Mongolia. Geological Bulletin of China 21, 584e591 (in Chinese, English abstract).

Ren, D., Shih, C.K., Gao, T.-P., Yao, Y.-Z., Zhao, Y.-Y., 2010. Silent stories-insect fossil treasures from Dinosaur Era of the northeastern China. Science Press, Beijing, 322pp.

Shen, Y.-B., Chen, P.-J., Huang, D.-Y., 2003. Age of the fossil conchostracans from Daohugou of Ningcheng, Inner Mongolia. Journal of Stratigraphy 27, 311e313 (in Chinese, English abstract).

Stigall, A.L., Hartman, J.H., 2008. A new spinicaudatan genus (Crustacea:'Conchostraca') from the Late Cretaceous of Madagascar. Palaeontology 51, 1053e1067.

Stigall, L.A., Babcock, E.L., Briggs, D.E.G., Leslie, S.A., 2008. Taphonomy of lacustrine interbeds in the Kirkpatrick Basalt (Jurassic), Antarctica. PALAIOS 23, 344e355.

Stigall, A.L., Hembree, D.I., Gierlowski-Kordesch, E.H., Weismiller, H.C., 2014. Evidence for a dioecious mating system in Early Jurassic Hardapestheria maxwelli gen. et sp. nov. (Crustacea, Branchiopoda, Spinicaudata) from the Kalkrand Formation of Namibia. Palaeontology 57, 127e140.

Stigall, A.L., Plotnick, R.E., Park Boush, L.E., 2017. The first Cenozoic spinicaudatans from North America. Journal of Paleontology 91, 467e476.

Sullivan, C., Wang, Y., Hone, D.W.E., Wang, Y.-Q., Xu, X., Zhang, F.-C., 2014. The vertebrates of the Jurassic Daohugou Biota of northeastern China. Journal of Vertebrate Paleontology 34, 243e280.
Sullivan, C., Xu, X., O'Connor, J.K., 2017. Complexities and novelties in the early evolution of avian flight, as seen in the Mesozoic Yanliao and Jehol biotas of Northeast China. Palaeoworld 26, 212e229.
Tan, J.-J., Ren, D., 2002. Palaeoecology of insect community from Middle Jurassic Jiulongshan Formation in Ningcheng County, Inner Mongolia, China. Acta Zootaxonomica Sinica 27, 428e434.
Tasch, P., 1982. Experimental valve geothermometry applied to fossil conchostracan valves, Blizzard Heights, Antarctica. In: Craddock, C. (Ed.), Antarctic geoscience. University of Wisconsin Press, Madison, pp. 661e668.
Vannier, J., Thiéry, A., Racheboeuf, P.R., 2003. Spinicaudatans and ostracods (Crustacea) from the Montceau Lagerstätte (Late Carboniferous, France): morphology and palaeoenvironmental significance. Palaeontology 46, 999e1030.
Wang, B., Li, J.-F., Fang, Y., Zhang, H.-C., 2008. Preliminary elemental analysis of fossil insects from the Middle Jurassic of Daohugou, Inner Mongolia and its taphonomic implications. Science Bulletin 54, 783e787.
Wang, B., Zhao, F.-C., Zhang, H.-C., Fang, Y., Zheng, D.-R., 2012. Widespread pyritization of insects in the Early Cretaceous Jehol Biota. PALAIOS 27, 707e711.
Wang, X.-L., Wang, Y.-Q., Zhang, F.-C., Zhang, J.-Y., Zhou, Z.-H., Jin, F., Hu, Y.-M., Gu, G., Zhang, H.-C., 2000. Vertebrate biostratigraphy of the lower Cretaceous Yixian Formation in Lingyuan, western Liaoning and its neighboring southern Nei Mongol (Inner Mongolia), China. Vertebrata Palasiatica 38, 95e101 (in Chinese, English abstract).
Wu, F.-Y., Xu, Y.-G., Gao, S., Zheng, J.-P., 2008. Lithospheric thinning and destruction of the North China Craton. Acta Petrologica Sinica 24, 1145e1174 (in Chinese, English abstract).
Xu, X., Zhou, Z.-H., Sullivan, C., Wang, Y., Ren, D., 2016. An Updated Review of the Middle-Late Jurassic Yanliao Biota: Chronology, Taphonomy, Paleontology and Paleoecology. Acta Geologica Sinica-English Edition 90, 2229e2243.
Yang, W., Li, S.-G., 2008. Geochronology and geochemistry of the Mesozoic volcanic rocks in Western Liaoning: implications for lithospheric thinning of the North China Craton. Lithos 102, 88e117.
Yang, Z.-X., Wang, S.-Y., Tian, Q.-Y., Wang, B., Hethke, M., McNamara, M.E., Benton, M.J., Xu, X., Jiang, B.-Y., 2019. Palaeoenvironmental reconstruction and biostratinomic analysis of the Jurassic Yanliao Lagerstätte in northeastern China. Palaeogeography, Palaeoclimatology, Palaeoecology 514, 739e753.
Zhang, W.-T., Chen, P.-C., Shen, Y.-B., 1976. Fossil Conchostraca of China. Science Press, Beijing, 325pp (in Chinese).
Zhou, Z.-H., 2006. Evolutionary radiation of the Jehol Biota: chronological and ecological perspectives. Geological Journal 41, 377e393.
Zhou, Z.-H., 2014. The Jehol Biota, an Early Cretaceous terrestrial Lagerstätte: new discoveries and implications. National Science Review 1, 543e559.
Zhou, Z.-H., Barrett, P.M., Hilton, J., 2003. An exceptionally preserved Lower Cretaceous ecosystem. Nature 421, 807e814.
Zhou, Z.-H., Wang, Y., 2017. Vertebrate assemblages of the Jurassic Yanliao Biota and the Early Cretaceous Jehol Biota: Comparisons and implications. Palaeoworld 26, 241e252.

Appendix A. Supplementary data

Supplementary data to this article can be found online at https://doi.org/10.1016/j.cretres.2019.01.025.